Pharmacokinetic Evaluation of [11C]CEP-32496 in Nude Mice Bearing BRAF V600E Mutation-Induced Melanomas

Cuiping Jiang, MMSc[1,2], Lin Xie, MD, PhD[1], Yiding Zhang, BSc[1], Masayuki Fujinaga, PhD[1], Wakana Mori, MSc[1], Yusuke Kurihara, PhD[1], Tomoteru Yamasaki, PhD[1], Feng Wang, MD, PhD[2], and Ming-Rong Zhang, MD, PhD[1]

Abstract

CEP-32496, also known as RXDX-105 or Agerafenib, is a new orally active inhibitor for the mutated v-raf murine sarcoma viral oncogene homolog B1 (BRAF V600E), which has attracted considerable attention in clinical trials for the treatment of human cancers. Here, we used carbon-11-labeled CEP-32496 ([11C]CEP-32496) as a positron emission tomography (PET) radiotracer to evaluate its pharmacokinetic properties and explore its potential for in vivo imaging. Following radiotracer synthesis, we performed in vitro binding assays and autoradiography of [11C]CEP-32496 in the A375 melanoma cell line and on tumor tissue sections from mice harboring the BRAF V600E mutation. These were followed by PET scans and biodistribution studies on nude mice bearing subcutaneous A375 cell-induced melanoma. [11C]CEP-32496 showed high binding affinity for BRAF V600E-positive A375 melanoma cells and densely accumulated in the respective tissue sections; this could be blocked by the BRAF V600E selective antagonist sorafenib and by unlabeled CEP-32496. The PET and biodistribution results revealed that [11C]CEP-32496 accumulated continuously but slowly into the tumor within a period of 0 to 60 minutes postinjection in A375-melanoma-bearing nude mice. Metabolite analysis showed high in vivo stability of [11C]CEP-32496 in plasma. Our results indicate that [11C]CEP-32496 has excellent specificity and affinity for the BRAF V600E mutation in vitro, while its noninvasive personalized diagnostic role needs to be studied further.

Introduction

The proto-oncogene v-raf murine sarcoma viral oncogene homolog B1 (BRAF) is a major signal transducer and one of the most frequently mutated genes in human cancers. It has been identified in approximately 7% of all cancers but is most frequently associated with melanoma (60%-70%), as well as with papillary thyroid (29%-83%), colorectal (4%-16%), and ovarian (5%-13%) carcinomas.[1-3] A single amino acid mutation in the protein, of valine to glutamate (V600E), is found in the vast majority of cases. This mutation constitutes a BRAF kinase–activating mutation, which confers a transforming and immortalization potential to tumor cells, thus resulting in uncontrolled proliferation and inhibition of differentiation.[4-6] In recent years, inhibition of V600E-mutated BRAF (BRAF V600E) has been the "poster child" of precision medicine paradigms for molecularly targeted therapeutics in solid malignancies.[1,7,8]

BRAF V600E kinase inhibitors, such as sorafenib, vemurafenib, and dabrafenib, constitute a great breakthrough in current targeted therapy. They have higher response rates and lead to

[1] Department of Radiopharmaceuticals Development, National Institute of Radiological Sciences, National Institutes for Quantum and Radiological Science and Technology, Chiba, Japan
[2] Department of Nuclear Medicine, Nanjing First Hospital, Nanjing Medical University, Nanjing, China

Corresponding Authors:
Feng Wang, Department of Nuclear Medicine, Nanjing First Hospital, Nanjing Medical University, Nanjing 210029, China.
Email: fengwangcn@hotmail.com
Ming-Rong Zhang, Department of Radiopharmaceuticals Development, National Institute of Radiological Sciences, National Institutes for Quantum and Radiological Science and Technology, Chiba 8555, Japan.
Email: zhang.ming-rong@qst.go.jp
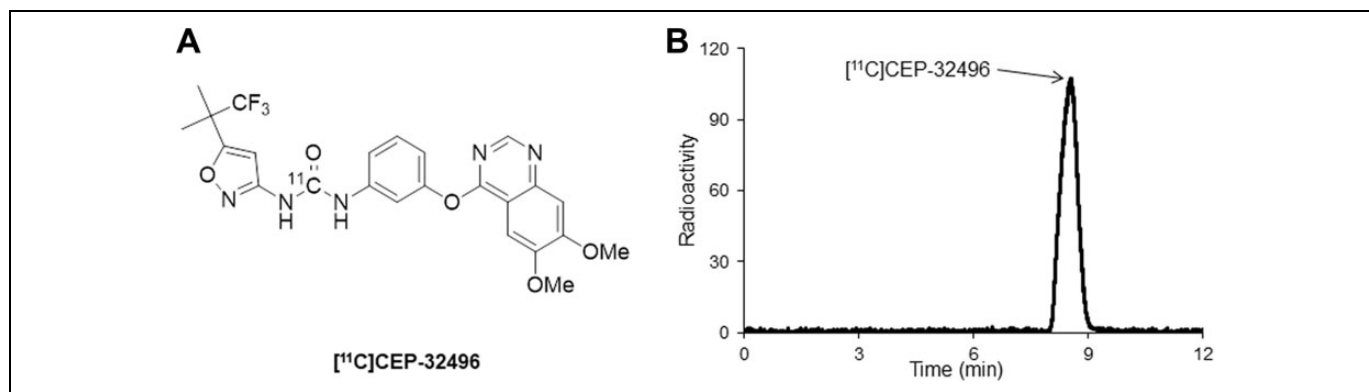
Figure 1. Chemical structure (A) of [¹¹C]CEP-32496 and a typical high performance liquid chromatography radioactive chromatogram (B) of the formulated [¹¹C]CEP-32496 product.

significantly longer overall survival than traditional cytotoxic chemotherapy.[8-10] However, patients commonly develop resistance to targeted therapy with these drugs, with an average time of approximately 7 months,[11,12] thus increasing the need for developing new generation BRAF[V600E] inhibitors. In regard to exploring new avenues, a crucial challenge is to facilitate the rapid evaluation of these potential targeted agents and optimize their application. The technology of functional positron emission tomography (PET) imaging, in combination with the development of targeted radiotracers, exhibits great potential toward accelerating drug development, by allowing the noninvasive testing of the possible therapeutic agents at earlier stages in vivo.

CEP-32496, otherwise known as RXDX-105 or Agerafenib [1-(3-(6,7-dimethoxyquinazolin-4-yloxy)phenyl)-3-(5-(1,1,1-trifluoro-2-methylpropan -2-yl)isoxazol-3-yl)urea hydrochloride], is a relatively novel pharmacologically active BRAF[V600E] inhibitor, which potently inhibits the phosphorylation of mitogen-activated protein kinase (MAPK) kinase.[13,14] In vitro, CEP-32496 inhibits proliferation and exhibits selective cytotoxicity in cells harboring the BRAF[V600E] mutation, but not in wild-type cells.[13,14] In preclinical studies of BRAF[V600E]-mutant melanoma xenografts, the oral administration of CEP-32496 (30-100 mg/kg, twice daily) was shown to lead to tumor stasis and regression, without any adverse effects. Currently, CEP-32496 is being tested in clinical trials in patients with advanced solid tumors (phase 1/1b, NCT01877811).[15] Safety profile analysis indicates that CEP-32496 is tolerable at doses of up to 350 mg/d and demonstrates antitumor activity in some patients.[16]

Previously, in order to noninvasively probe the pharmacokinetic efficiency of CEP-32496 in vivo, we developed carbon-11-labeled CEP-32496 ([¹¹C]CEP-32496; Figure 1) as a PET radiotracer and characterized the role of the P-glycoprotein/breast cancer resistance protein (P-gp/BCRP) on the efflux of [¹¹C]CEP-32496.[17] In the present study, to promote future development of personalized therapies with CEP-32496, we evaluated the pharmacokinetics of [¹¹C]CEP-32496 and explored its potential for in vivo imaging in nude mice bearing BRAF[V600E]-mutant melanoma.

Material and Methods

Radiosynthesis of [¹¹C]CEP-32496

[¹¹C]CEP-32496 (Figure 1A) was produced using [¹¹C]phosgene ([¹¹C]COCl$_2$) as a radiolabeling agent, as previously described.[17] We started with 22 to 23 GBq of [¹¹C]CO$_2$ and obtained 0.70 to 1.34 GBq (n = 15) of [¹¹C]CEP-32496 at the end of synthesis (EOS). The averaged radiochemical yield of [¹¹C]CEP-32496 was 15% ± 4.5%, based on [¹¹C]CO$_2$, decay corrected at the end of bombardment. The radiochemical purity (Figure 1B) and molar activity of [¹¹C]CEP-32496 were >98% and 40 to 85 GBq/μmol (n = 15) at EOS, respectively. The analytical results complied with our in-house quality control and safety specifications for animal experiments.

Measurement of Lipophilicity

A mixture of [¹¹C]CEP-32496 (radiochemical purity: >99%; around 150 000 counts per minute [cpm]), *n*-octanol (3.0 g), and phosphate-buffered saline (PBS; 3.0 g, 0.1 M, pH 7.4) in a test tube was vortexed for 3 minutes at room temperature, followed by centrifugation at 3500*g* for 5 minutes. An aliquot of 0.65 mL PBS and 0.65 mL *n*-octanol was removed and weighed and its radioactivity was counted with a 1480 Wizard autogamma counter (PerkinElmer, Waltham, Massachusetts), respectively. The logD value was calculated by comparing the ratio of cpm/g of *n*-octanol to that of PBS and expressed as logD = log[cpm/g (*n*-octanol)/cpm/g (PBS)]. All measurements were performed in triplicate.

Cell Lines and Mouse Models

The human melanoma cell line A375 (American Type Culture Collection, Manassas, Virginia), carrying the BRAF[V600E] mutation,[18] was maintained and passaged in Dulbecco's Modified Eagle's Medium (DMEM) supplemented with 10% fetal bovine serum, sodium pyruvate, 1 mM penicillin (100 U/mL), and 0.1 mg/mL streptomycin.

The animal studies were approved by the Animal Ethics Committee of the National Institutes for Quantum and

Radiological Science and Technology. The animals were maintained and handled in accordance with the recommendations of the National Institute of Health and the institutional guidelines of the National Institutes for Quantum and Radiological Science and Technology. Animal experiments were performed in 6- to 8-week-old Balb/c nude female mice (Japan SLC, Shizuoka, Japan). A375-melanoma-bearing nude mice were generated by injecting a single-cell suspension of 1×10^6 A375 cells (in 50 μL serum-free DMEM, mixed with 50 μL Matrigel) subcutaneously into the left flank. Nineteen days after inoculation, mice with a maximum tumor diameter of 9 to 12 mm were selected for further studies. All the following in vivo experiments were performed with 4 mice per experimental group.

In Vitro Binding Assays

To examine the cellular affinity of [^{11}C]CEP-32496, A375 cells were seeded in 24-well plates (1×10^5 cells/well) and allowed to attach overnight. [^{11}C]CEP-32496 (3.7 MBq/well) was added to the cultures, in combination with different concentrations of the unlabeled CEP-32496 (0-10^3 μM) or the BRAF^{V600E} selective antagonist sorafenib (0-10^3 μM), for 1 hour at 37°C, and the cells were washed and dissolved in 0.2 M NaOH. The radioactivity was measured using a γ-counter (PerkinElmer). The protein content of the cell lysate was quantified by using the Bio-Rad protein assay kit (Bio-Rad, Hercules, California). We calculated cellular uptake as the ratio of incorporated radioactivity over protein content (in milligrams). The IC$_{50}$ values of the [^{11}C]CEP-32496 uptake were calculated by performing nonlinear regression analysis, using Prism 5 (GraphPad Software, La Jolla, California).

Pharmacokinetic Imaging by PET

Positron emission tomography scans were performed using a small animal Siemens Inveon PET scanner (Siemens, Knoxville, Tennessee), which provides 159 transaxial slices, with 0.796-mm (center-to-center) spacing, 10-cm transaxial field of view (FOV), and 12.7-cm axial FOV. Emission scans were acquired in the 3-dimensional list mode, with an energy window of 350 to 650 keV. Imaging was performed under isoflurane anesthesia at 0 to 60 minutes after an intravenous injection of [^{11}C]CEP-32496 (16.0-20.4 MBq/0.1 mL) via a lateral tail vein in the A375-melanoma-bearing nude mice. In order to improve tumor penetration by [^{11}C]CEP-32496, the P-gp/BCRP inhibitor GF-120918 (10 mg/kg) was administered 5 minutes before the [^{11}C]CEP-32496 injection. This was previously reported to increase the intracellular drug accumulation and reverse the BCRP-mediated multidrug resistance.[19] All list-mode acquisition data were sorted into 3-dimensional sinograms, which were then Fourier-rebinned into 2-dimensional sinograms (4×1, 8×2, and 8×5 frames $\times$ minutes), and corrected for the decay of the radiotracer. Dynamic images were reconstructed from 3-dimensional sonogram-filtered back

projections, by using a Hanning filter, with a Nyquist cutoff of 0.5 cycles/pixel.

Regions of interest (ROIs) in the heart, liver, kidney, brain, and tumor were drawn in the PET images by manual outlining the organs and tissues throughout the image slices by using the Siemens Inveon Research Workplace 4.0 software. The average radioactivity concentration was obtained by calculating the ratio of the mean pixel value (intensity) to the volume of the selected ROI. Regional radioactivity uptake was decay-corrected relative to the injection time, normalized to body weight, and expressed as the percentage of the injected dose per gram (%ID/g). Time–activity curves (TACs) of [^{11}C]CEP-32496 in individual organs and tumor were determined.

Biodistribution Studies

A375-melanoma-bearing nude mice were killed by cervical dislocation at 30 and 60 minutes after [^{11}C]CEP-32496 (6.6 MBq/0.1 mL) injection. Blood, heart, lung, liver, pancreas, spleen, kidney, small intestine, large intestine, skin, muscle, brain, and tumor were promptly excised, harvested, and weighed. Radioactivity was counted using the γ-counter and expressed as a percentage of the injected dose per gram of wet tissue (%ID/g). All radioactivity measurements were corrected for decay.

In Vivo Stability Analysis

Balb/c nude mice were injected with [^{11}C]CEP-32496 (12.6-13.0 MBq/0.25 mL) via a lateral tail vein. The mice were killed by cervical dislocation at 5 and 30 minutes after the radiotracer injection. Urine was rapidly taken. Blood was collected and centrifuged at 15 000 rpm for 2 minutes at 4°C to separate the plasma. Urine and plasma were deproteinized and the supernatant was collected. An aliquot of the supernatant (0.3-0.6 mL) obtained from the plasma or urine was injected into an high performance liquid chromatography (HPLC) system with a radioactivity detector and analyzed using a Capcell Pak C$_{18}$ column (4.6 mm internal diameter $\times$ 250 mm, SHISEIDO, Tokyo, Japan) with acetonitrile/H$_2$O (6/4, vol/vol) at a flow rate of 1 mL/min. The percentage ratio of [^{11}C]CEP-32496 (retention time $=$ 8.3 minutes) to total radioactivity (corrected for decay) on the HPLC chromatogram was calculated as $\% =$ (peak area for radiotracer/total peak area) $\times$ 100.

In Vitro Autoradiography

A375-melanoma-bearing nude mice were euthanized, the tumor grafts were removed, and frozen sections (5 μm) were prepared. After preincubation in 50 mM Tris buffer for 20 minutes at room temperature, sections were incubated in fresh Tris buffer, containing [^{11}C]CEP-32496 (11.6 MBq/L) for 30 minutes at 25°C. Displacement experiments were performed by coincubation with 10 μM of either sorafenib or unlabeled CEP-32496, added to the [^{11}C]CEP-32496-containing incubation solution. After incubation, sections were washed with cold Tris

buffer (3×5 minutes), immersed in cold distilled water, and dried with cold air. Subsequently, sections were exposed to the BAS-MS 2325 imaging plate (Fujifilm, Tokyo, Japan) for 30 minutes and analyzed with the BAS 5000 Bio Imaging Analyzer System (Fujifilm). Radioactivity in tumor sections was quantified and expressed as the photostimulated luminescence per unit area (PSL/mm^2).

Statistical Analysis

All data are presented as the mean of the values $\pm$ the standard error of mean. Intergroup comparisons were performed using the 1-way analysis of variance test. The threshold for statistical significance was set at $P < .05$. All in vivo experimental results included data from 4 mice per group, and all in vitro results represent data from 3 independent experiments, in which the mean ratio of 3 replicates per experiment was calculated.

Results

Lipophilicity

We measured the log D value of $[^{11}C]CEP$-32496 using liquid–liquid partition between *n*-octanol and PBS ("shake flask method"). $[^{11}C]CEP$-32496 exhibited a high lipophilicity, with the logD value of 4.4.

In Vitro Binding Assays

The A375 melanoma cell line carries the BRAF^{V600E} mutation, which is sensitive to BRAF-specific inhibitors. The cellular binding affinity of $[^{11}C]CEP$-32496 was evaluated in cells that were incubated with $[^{11}C]CEP$-32496 and different concentrations of unlabeled CEP-32496 or sorafenib. In both cases, $[^{11}C]CEP$-32496 showed high binding affinity for the A375 melanoma cells, with IC_{50} values of 10.30 μM, in the case of treatment with unlabeled CEP-32496, and 6.41 μM, in the case of treatment with sorafenib (Figure 2).

Pharmacokinetic Imaging by PET

In order to visualize in vivo the pharmacokinetic properties of $[^{11}C]CEP$-32496, we performed dynamic PET in A375-melanoma-bearing nude mice during 0 to 60 minutes after administration of the radiotracer and sorafenib. Figure 3A shows images of typical $[^{11}C]CEP$-32496 pharmacokinetics. Sixty minutes after radiotracer injection, the overall delivery of $[^{11}C]CEP$-32496 to targeted A375 xenografts did not seem sufficient to be visualized by this noninvasive imaging. The TACs showed slow accumulation of $[^{11}C]CEP$-32496 in the tumor, ranging from 0.19 ± 0.03 %ID/g to 0.69 ± 0.08 %ID/g, in a period of 0 to 60 minutes postinjection (Figure 3B). One minute after injection, $[^{11}C]CEP$-32496 was carried through the vena cava to the heart, liver, and kidney, followed by a rapid distribution throughout the whole body (Figure 3A and B). Thereafter, PET revealed that $[^{11}C]CEP$-32496 flowed from the liver to the small intestine within 60 minutes after
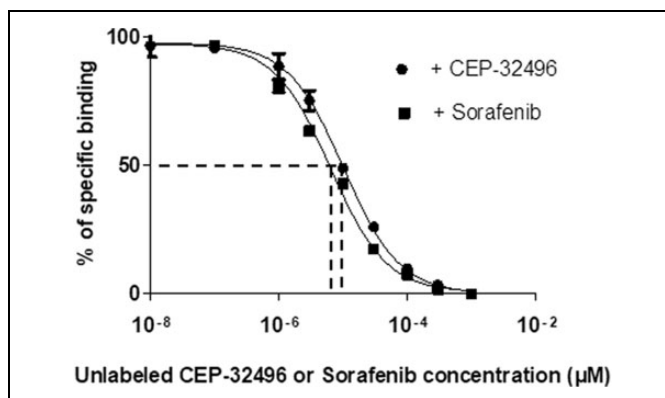
Figure 2. Binding affinity of $[^{11}C]CEP$-32496 in BRAF^{V600E}-positive melanoma cells. The IC_{50} values of $[^{11}C]CEP$-32496 uptake were calculated by nonlinear regression analysis using Prism 5. The binding assay of $[^{11}C]CEP$-32496 was performed with different concentrations (0-10^3 μM) of unlabeled CEP-32496 or sorafenib. Data are expressed as means $\pm$ standard error of mean (SEM), based on 3 independent experiments.

injection, suggesting that $[^{11}C]CEP$-32496 was excreted by the hepatobiliary system and intestine. Negligible radioactivity was observed in the brain during 60 minutes (Figure 3A and B).

Ex Vivo Biodistribution

To validate the results of the in vivo pharmacokinetic imaging, we measured the radioactivity biodistribution in the main organs and tissues at 30 and 60 minutes after injection with $[^{11}C]CEP$-32496 (Table 1). In line with the PET results, the radioactivity uptake was highest in the liver and small intestine, compared to the rest of the body, at 30 minutes (liver, 19.08 ± 1.23 %ID/g; small intestine, 33.79 ± 1.23 %ID/g) and 60 minutes (liver, 25.23 ± 0.57 %ID/g; small intestine, 22.30 ± 3.18 %ID/g) after $[^{11}C]CEP$-32496 injection, which confirmed that most of the radiotracer was excreted from the hepatobiliary system and intestine. Sustained but low levels of radioactivity were detected in the tumor at 30 minutes (1.79 ± 0.07 %ID/g) and 60 minutes (1.85 ± 0.09 %ID/g) after administration. Taken together, the ex vivo biodistribution and PET analysis suggest that $[^{11}C]CEP$-32496 concentration was not adequate for its sensitive visualization in the A375 melanoma.

Positron Emission Tomography Tumor Imaging After Pretreatment With a Drug Efflux Transporter Inhibitor

It is known that the BRAF^{V600E} inhibitor sorafenib is a substrate for the drug efflux transporter system P-gp/BCRP.[20-22] To explore the influence of this system on $[^{11}C]CEP$-32496 accumulation in the tumor and improve $[^{11}C]CEP$-32496 tumor penetration, we blocked P-gp/BCRP by injecting an excess of the P-gp/BCRP inhibitor GF-120918 (10 mg/kg), 5 minutes before $[^{11}C]CEP$-32496 injection. The uptake of radioactivity in targeted xenografts increased slowly during the first 25 minutes after $[^{11}C]CEP$-32496 injection, while 60 minutes after it reached higher values in GF-120918-treated than in untreated mice,
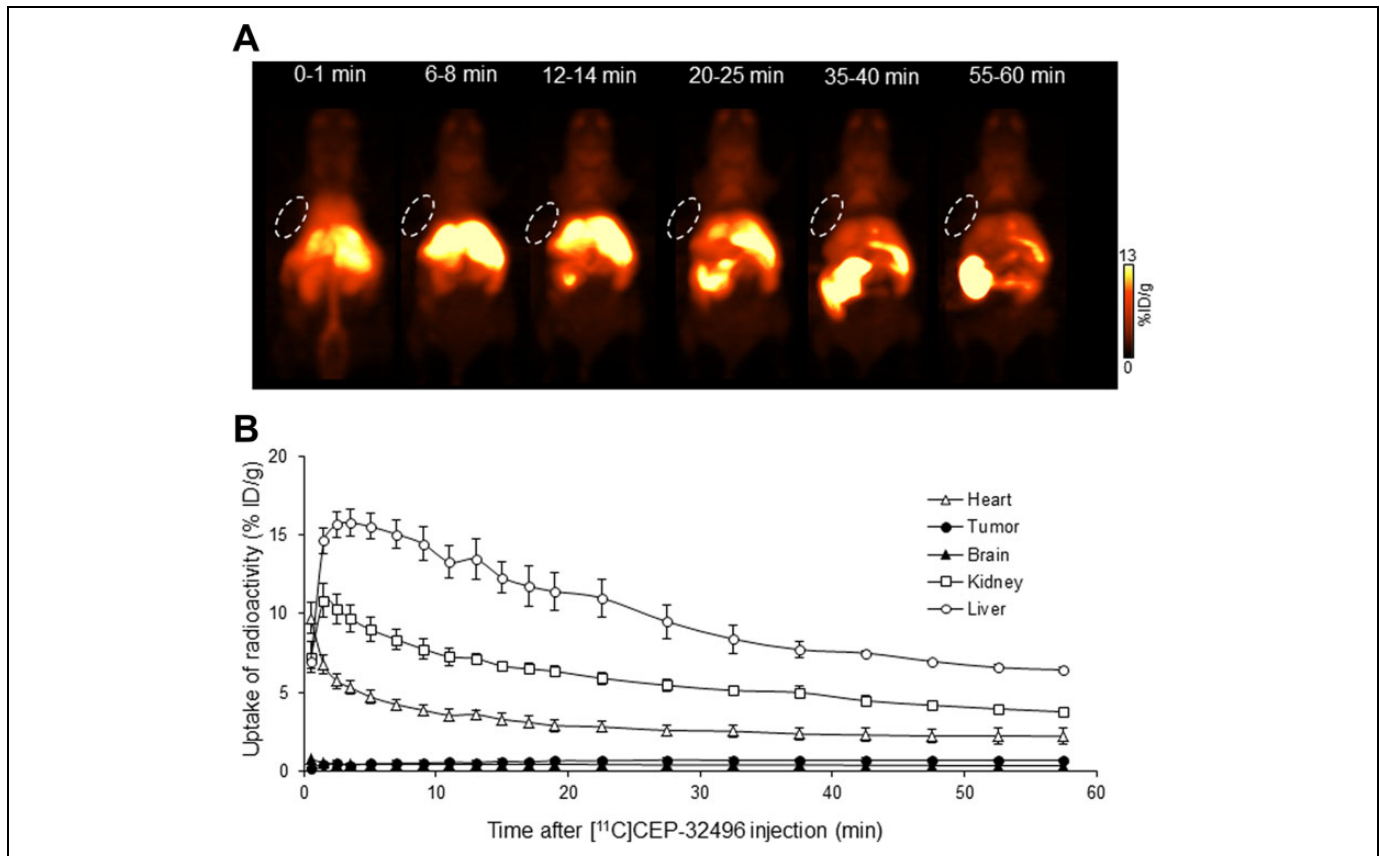
Figure 3. Representative pharmacokinetic images and quantification of [^{11}C]CEP-32496 in nude mice-bearing A375 xenografts. A, Representative maximum intensity projection images summed from scans during different time points after [^{11}C]CEP-32496 injection. White circles indicate tumors. B, Time–activity curves (TACs) of [^{11}C]CEP-32496 in the heart, tumor, brain, kidney, and liver. Data are expressed as means $\pm$ standard error of mean (SEM) from 4 tumor-bearing mice per group.

Table I. Biodistribution of [^{11}C]CEP-32496 Radioactivity at 30 and 60 Minutes After the Radiotracer Injection in Nude Mice-Bearing BRAF^{V600E}-Mutation Melanoma.[a]

Tissue	30 Minutes	60 Minutes
Blood	1.75 $\pm$ 0.45	1.31 $\pm$ 0.02
Heart	3.33 $\pm$ 0.11	4.69 $\pm$ 0.20
Lung	3.45 $\pm$ 0.20	5.16 $\pm$ 0.34
Liver	19.08 $\pm$ 0.71	25.23 $\pm$ 0.57
Pancreas	5.24 $\pm$ 0.19	6.97 $\pm$ 0.33
Spleen	2.20 $\pm$ 0.07	3.35 $\pm$ 0.15
Kidney	6.82 $\pm$ 0.27	9.77 $\pm$ 0.45
Small intestine	33.79 $\pm$ 1.23	22.30 $\pm$ 3.18
Large intestine	4.88 $\pm$ 0.25	3.44 $\pm$ 0.22
Skin	2.45 $\pm$ 0.09	2.57 $\pm$ 0.18
Tumor	1.79 $\pm$ 0.07	1.85 $\pm$ 0.09
Muscle	2.03 $\pm$ 0.11	2.63 $\pm$ 0.05
Brain	0.13 $\pm$ 0.00	0.15 $\pm$ 0.00

[a]Data are expressed as the mean %ID/g tissue with the standard error of mean (n = 4 mice/group).

although the differences were not statistically significant. Figure 4 summarizes the TACs of [^{11}C]CEP-32496 in A375 melanoma in the 2 groups of mice (treated with GF-120918 and untreated).

In Vivo Stability Analysis

To explore potential reasons about in vivo low uptake of [^{11}C]CEP-32496, the stability of the radiotracer was assessed by investigating the radiolabeled metabolites in plasma and urine of the nude mice. As shown in Table 2, radio-HPLC analysis showed that 92.18% (at 5 minutes; Figure 5A) and 87.78% (at 30 minutes; Figure 5B) of total radioactivity in the plasma represented the intact form, whereas 88.11% and 98.02% of total radioactivity represented the radiolabeled metabolites in the urine at 5 and 30 minutes, respectively, after the injection of [^{11}C]CEP-32496.

In Vitro Autoradiography

To furtherly check the targeting potential of [^{11}C]CEP-32496 for the BRAF^{V600E} tumor, we determined tissue binding by performing in vitro autoradiography in sections from A375 melanomas. We observed dense radioactivity in A375 melanoma (347.29 $\pm$ 8.24 PSL/mm^2), while we detected only minimum radioactivity in sections that were additionally treated with sorafenib (10.50 $\pm$ 0.31 PSL/mm^2) or unlabeled CEP-32496 (12.759 $\pm$ 0.40 PSL/mm^2; Figure

6). Quantitative results showed that sorafenib and unlabeled CEP-32496 significantly blocked [^{11}C]CEP-32496 uptake in the tumor slices ($P < .01$). These results, in combination with our results using the A375 melanoma cell line (Figure 2B), demonstrate the high in vitro specificity of [^{11}C]CEP-32496 to BRAF^{V600E}.
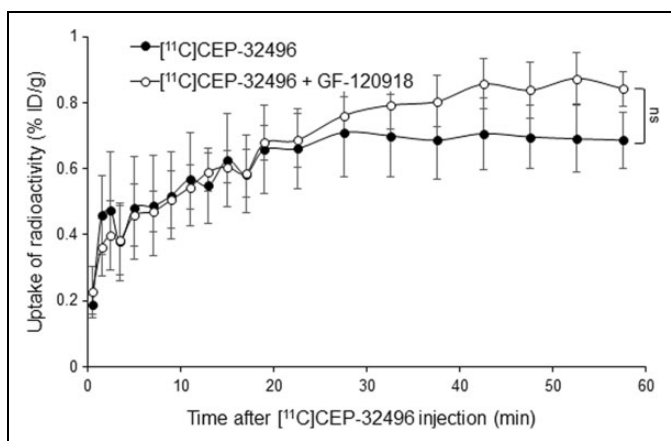
Figure 4. Quantification of [^{11}C]CEP-32496 in A375 xenografts. Time–activity curves (TACs) of [^{11}C]CEP-32496 in mice preinjected with and without the P-glycoprotein/breast cancer resistance protein inhibitor GF-120918. Data are expressed as means ± standard error of mean (SEM) from 4 tumor-bearing mice per group. Comparisons were performed using 1-way analysis of variance test. ns indicates no statistically significant.

Discussion

In this study, we systematically evaluated the pharmacokinetic characteristics of [^{11}C]CEP-32496 and explored the potential of this radiotracer with PET imaging in nude mice bearing BRAF^{V600E} melanoma.

The majority of melanomas express the BRAF^{V600E} mutation, which results in the constitutive activation of the MAPK pathway and in uncontrolled cellular growth.[23] This mutation has received much attention as an important target for personalized diagnosis and treatment of melanoma, while single-agent therapies have demonstrated clinical effects.[2,6,8,24] Preclinical studies have shown that CEP-32496 is orally bioactive in multiple preclinical species and has a high antitumor ability against BRAF^{V600E}-positive carcinoma xenografts in nude mice.[13] The antitumor activity of CEP-32496 in patients with BRAF^{V600E}-positive multiple cancers treated has also been reported in clinical trials.[16] In this study, we showed that under in vitro conditions, CEP-32496 strongly binds BRAF^{V600E}-positive A375 melanoma tissues and that this binding is significantly blocked by the BRAF^{V600E} selective antagonist sorafenib, as well as by unlabeled CEP-32496. These in vitro results verify the high binding affinity of CEP-32496 for the BRAF^{V600E} mutation in melanomas.

Dynamic PET imaging with radiotracers has been commonly used to temporally and spatially track the in vivo course of drugs and is a powerful modality to discover novel therapeutic strategies, due to its excellent capacity in capturing drug molecules in vivo, noninvasively, and in a timely manner.[25] This quantitative, imaging-based pharmacokinetic study

Table 2. In Vivo Stability Analysis of [^{11}C]CEP-32496 in the Plasma and Urine of the Nude Mice.[a]

	Plasma			Urine		
Time After Injection	Radioactivity (%ID/g)	Intact (%)	Metabolites (%)	Radioactivity (%ID/g)	Intact (%)	Metabolites (%)
5 minutes	3.69 ± 0.35	92.18 ± 0.26	7.82 ± 0.26	1.59 ± 0.43	11.89 ± 2.62	88.11 ± 2.62
30 minutes	1.50 ± 0.11	87.78 ± 0.45	12.21 ± 0.45	6.34 ± 0.78	1.98 ± 0.79	98.02 ± 0.79

[a]Data are expressed as %ID/g tissue or % of tailored radioactivity (means ± standard error of mean; n = 4 mice/group). The ratios of radioactivity in the plasma extracting from the blood were 61.11% ± 6.41% at 5 minutes and 93.74% ± 2.03% at 30 minutes after [^{11}C]CEP-32496 injection.
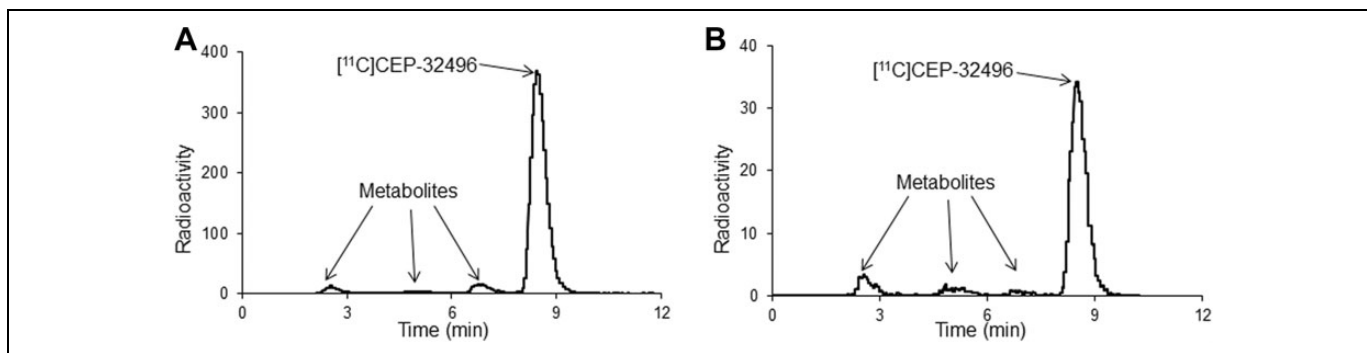
Figure 5. Representative high performance liquid chromatography chromatograms for the plasma of Balb/c nude mice after [^{11}C]CEP-32496 injection. Radio-HPLC analysis showed that 92.18% at 5 minutes (A) and 87.78% at 30 minutes (B) of total radioactivity in the plasma represented the intact form.
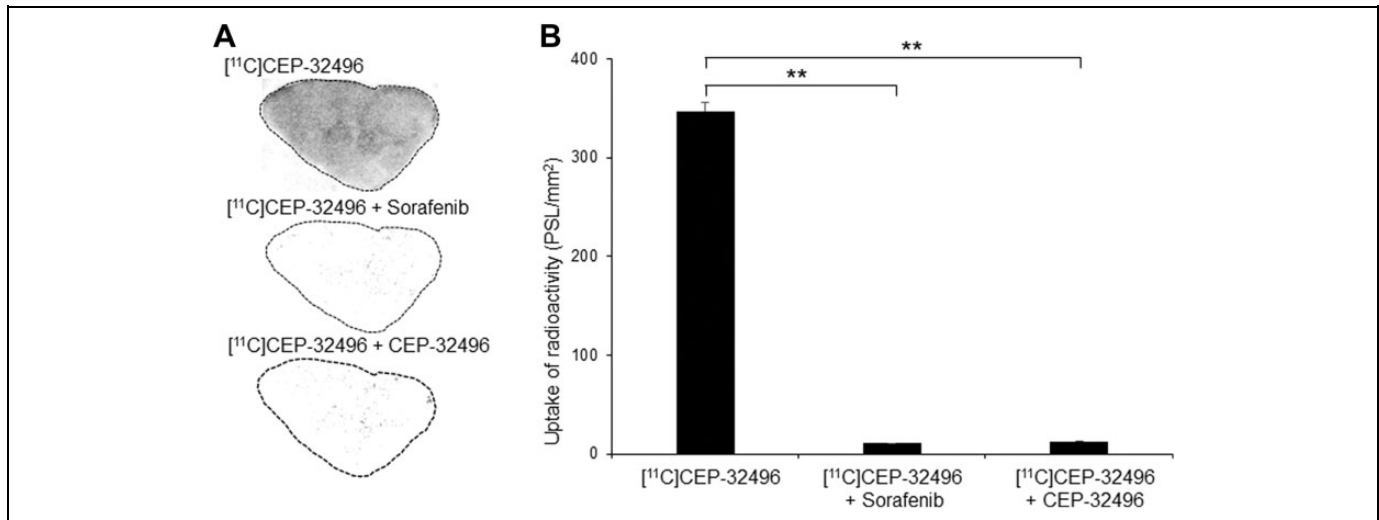
Figure 6. [^{11}C]CEP-32496 binding in BRAF^{V600E}-positive A375-tumor tissue sections. A, In vitro autoradiograms. Dense radioactivity of [^{11}C]CEP-32496 is present in A375 xenografts. The BRAF^{V600E} antagonist sorafenib or unlabeled CEP-32496 specifically blocked the uptake of [^{11}C]CEP-32496. B, Quantification of radioactivity levels in the autoradiograms. Intergroup comparisons were performed using 1-way analysis of variance test. Asterisks indicate statistical significance (**P < .01). Data are expressed as means $\pm$ standard error of mean (SEM), based on 3 independent experiments.

represents an exciting innovation in drug development.[26] Using dynamic PET imaging with [^{11}C]CEP-32496, we evaluated its pharmacokinetic characteristics. [^{11}C]CEP-32496 was carried through the circulation into the heart very quickly after injection and thereafter was removed rapidly via hepatobiliary, intestinal, and renal clearance. Unfortunately, we did not find an adequate tracer concentration for noninvasive imaging in the targeted A375 xenografts 60 minutes after [^{11}C]CEP-32496 injection. Our ex vivo biodistribution analysis verified the low uptake of [^{11}C]CEP-32496 in the tumor xenografts. The subsequent metabolite analysis verified that [^{11}C]CEP-32496 was highly stable in the plasma, so the low tumor uptake did not appear to be caused by the instability of the radiotracer.

Many factors influence the accumulation and retention of a radiotracer. For example, lipophilicity, drug efflux transporters, like P-gp/BCRP, remove the drug from cancer cells, thus causing drug resistance.[27,28] Although [^{11}C]CEP-32496 displayed excellent in vitro affinity and selectivity for BRAF^{V600E}, the in vivo PET and ex vivo biodistribution results indicated that the incorporation of [^{11}C]CEP-32496 in the A375 melanomas is not high. This discrepancy may be attributed to several factors; firstly, a too lipophilic compound can bind to the protein (eg, albumin) in the blood, limiting its penetrating into tumor cells. Thus, the high lipophilicity (logD = 4.4) of [^{11}C]CEP-32496 may be related to the low tumor uptake. Secondly, insufficient blood perfusion in the solid A375 melanoma may also contribute to the extremely low initial uptake of radioactivity after the [^{11}C]CEP-32496 injection. Thirdly, we used a very small dose "microdose" of radiotracer for the present PET imaging, and the uptake level of [^{11}C]CEP-32496 in A375 melanoma after the "microdose" administration might have been insufficient for in vivo visualization. Fourthly, the difference in the formulation and route of administration, to that of therapeutic goal of CEP-32496, could influence the bioavailability of the drug and limit the achievable concentration into the tumors, confronting the limits of translatability of the data in this context. Lastly, the presence of high levels of drug efflux transporters, such as the 2 representative ATP-binding cassette (ABC) transporters, BCRP and P-gp, which can actively remove the drug from cells, might limit the adsorption and distribution of the drug in the tumor cells and in the brain.[27,28] It has been shown that [^{11}C]CEP-32496 is a substrate for BCRP and/or P-gp and that these proteins limit the uptake of [^{11}C]CEP-32496 in the mouse brain, at the blood–brain barrier.[17] Therefore, this resistance mechanism might influence the accumulation of [^{11}C]CEP-32496 in the tumor, especially since we used only a microdose of the tracer. Indeed, preinjection with GF-120918, a third-generation inhibitor of ABC transporters, slightly increased the accumulation of [^{11}C]CEP-32496 in A375 melanoma. Therefore, the low radioactivity accumulation may be influenced by the drug efflux transport system.

Conclusions

This study demonstrated that [^{11}C]CEP-32496 has high tumor-binding efficiency, with excellent selectivity and specificity in vitro for BRAF^{V600E}-induced melanomas, which would be helpful for facilitating the development of BRAF^{V600E}-targeted therapy. Our in vivo studies showed that [^{11}C]CEP-32496 had gradual and slow accumulation into the targeted tumor, which did not ensure proper tumor accumulation of radiotracer to be visualized by the noninvasive PET imaging. The results presented here, in combination with the clinical data available regarding BRAF^{V600E}-mutation inhibition, may provide helpful information while performing the clinical trials of CEP-32496 in humans.

Author Contributions

CJ, LX contributed equally to this work.

References

1. Karoulia Z, Gavathiotis E, Poulikakos PI. New perspectives for targeting RAF kinase in human cancer. *Nat Rev Cancer*. 2017; 17(11):676–691.

2. Zambon A, Niculescu-Duvaz D, Niculescu-Duvaz I, Marais R, Springer CJ. BRAF as a therapeutic target: a patent review (2006-2012). *Expert Opin Ther Pat*. 2013;23(2):155–164.

3. Fiskus W, Mitsiades N. B-Raf inhibition in the clinic: present and future. *Ann Rev Med*. 2016;67:29–43.

4. Packer LM, East P, Reis-Filho JS, Marais R. Identification of direct transcriptional targets of (V600E)BRAF/MEK signalling in melanoma. *Pigment Cell Melanoma Res*. 2009;22(6):785–798.

5. Jakob JA, Bassett RL Jr, Ng CS, et al. NRAS mutation status is an independent prognostic factor in metastatic melanoma. *Cancer*. 2012;118(16):4014–4023.

6. Bucheit AD, Syklawer E, Jakob JA, et al. Clinical characteristics and outcomes with specific BRAF and NRAS mutations in patients with metastatic melanoma. *Cancer*. 2013;119(21):3821–3829.

7. Rosove MH, Peddi PF, Glaspy JA. BRAF V600E inhibition in anaplastic thyroid cancer. *N Eng J Med*. 2013;368(7):684–685.

8. Sosman JA, Kim KB, Schuchter L, et al. Survival in BRAF V600-mutant advanced melanoma treated with vemurafenib. *N Eng J Med*. 2012;366(8):707–714.

9. Holderfield M, Nagel TE, Stuart DD. Mechanism and consequences of RAF kinase activation by small-molecule inhibitors. *Br J Cancer*. 2014;111(4):640–645.

10. Corcoran RB, Atreya CE, Falchook GS, et al. Combined BRAF and MEK inhibition with dabrafenib and trametinib in BRAF V600-mutant colorectal cancer. *J Clin Oncol*. 2015;33(34):4023–4031.

11. Prahallad A, Sun C, Huang S, et al. Unresponsiveness of colon cancer to BRAF(V600E) inhibition through feedback activation of EGFR. *Nature*. 2012;483(7387):100–103.

12. Sun C, Wang L, Huang S, et al. Reversible and adaptive resistance to BRAF(V600E) inhibition in melanoma. *Nature*. 2014; 508(7494):118–122.

13. James J, Ruggeri B, Armstrong RC, et al. CEP-32496: a novel orally active BRAF(V600E) inhibitor with selective cellular and in vivo antitumor activity. *Mol Cancer Ther*. 2012;11(4):930–941.

14. Rowbottom MW, Faraoni R, Chao Q, et al. Identification of 1-(3-(6,7-dimethoxyquinazolin-4-yloxy)phenyl)-3-(5-(1,1,1-trifluoro-2-methylpropa n-2-yl)isoxazol-3-yl)urea hydrochloride (CEP-32496), a highly potent and orally efficacious inhibitor of V-RAF murine sarcoma viral oncogene homologue B1 (BRAF) V600E. *J Med Chem*. 2012;55(3):1082–1105.

15. Patel MR, Fakih M, Olszanski AJ, et al. A phase 1 dose escalation study of RXDX-105, an oral RET and BRAF inhibitor, in patients with advanced solid tumors. *J Clin Oncol*. 2016;34:2574–2574.

16. Li GG, Somwar R, Joseph J, et al. Antitumor activity of RXDX-105 in multiple cancer types with RET rearrangements or mutations. *Clin Cancer Res*. 2017;23(12):2981–2990.

17. Shimoda Y, Yui J, Fujinaga M, et al. [11C-carbonyl]CEP-32496: radiosynthesis, biodistribution and PET study of brain uptake in P-gp/BCRP knockout mice. *Bioorg Med Chem Lett*. 2014;24(15): 3574–3577.

18. Kang HB, Fan J, Lin R, et al. Metabolic rewiring by oncogenic BRAF V600E links ketogenesis pathway to BRAF-MEK1 signaling. *Mol Cell*. 2015;59(3):345–358.

19. Allen JD, van Loevezijn A, Lakhai JM, et al. Potent and specific inhibition of the breast cancer resistance protein multidrug transporter in vitro and in mouse intestine by a novel analogue of fumitremorgin C. *Mol Cancer Ther*. 2002;1(6):417–425.

20. Agarwal S, Sane R, Ohlfest JR, Elmquist WF. The role of the breast cancer resistance protein (ABCG2) in the distribution of sorafenib to the brain. *J Pharmacol Exp Ther*. 2011;336(1):223–233.

21. Asakawa C, Ogawa M, Kumata K, et al. [11C]sorafenib: radiosynthesis and preliminary PET study of brain uptake in P-gp/Bcrp knockout mice. *Bioorg Med Chem Lett*. 2011;21(8):2220–2223.

22. Poot AJ, van der Wildt B, Stigter-van Walsum M, et al. [11C]Sorafenib: radiosynthesis and preclinical evaluation in tumor-bearing mice of a new TKI-PET tracer. *Nucl Med Biol*. 2013;40(4):488–497.

23. McCubrey JA, Steelman LS, Chappell WH, et al. Roles of the Raf/MEK/ERK pathway in cell growth, malignant transformation and drug resistance. *Biochim Biophys Acta*. 2007;1773(8): 1263–1284.

24. Flaherty KT, McArthur G. BRAF, a target in melanoma: implications for solid tumor drug development. *Cancer*. 2010;116(21): 4902–4913.

25. Matthews PM, Rabiner EA, Passchier J, Gunn RN. Positron emission tomography molecular imaging for drug development. *Br J Clin Pharmacol*. 2012;73(2):175–186.

26. Xie L, Maeda J, Kumata K, et al. Development of 1-N-(11)C-Methyl-L- and -D-Tryptophan for pharmacokinetic imaging of the immune checkpoint inhibitor 1-Methyl-Tryptophan. *Sci Rep*. 2015;5:16417.

27. Gottesman MM, Fojo T, Bates SE. Multidrug resistance in cancer: role of ATP-dependent transporters. *Nat Rev Cancer*. 2002;2(1): 48–58.

28. de Vries NA, Zhao J, Kroon E, Buckle T, Beijnen JH, van Tellingen O. P-glycoprotein and breast cancer resistance protein: two dominant transporters working together in limiting the brain penetration of topotecan. *Clin Cancer Res*. 2007;13(21):6440–6449.